Local Hemodynamics and Intimal Hyperplasia at the Venous Side of Porcine Carotid Artery – Jugular Vein Shunt

Themistoklis A. Manos, Dimitrios P. Sokolis, Athina T. Giagini, Constantinos H. Davos, John D. Kakisis, Nikos Stergiopulos, Panayotis E. Karayannacos, Sokrates Tsangaris

Abstract—**One of the chief factors, incriminated for the formation of intimal hyperplasia at the venous side of an arteriovenous shunt (AVS), is the disturbed hemodynamic condition in that region. Owing to the difficulty of properly measuring the local flow field in AVS, numerical computation has been extensively used for its assessment. The purpose of this study was to examine the flow field in AVS with computational fluid dynamics (CFD). AVS was created in a pig between the common carotid artery and the internal jugular vein using an ePTFE graft. Input data to the computational model was obtained in vivo one month later, and adjacent vessels were excised and submitted to histological examination. The 3D geometry of the shunt was determined using biplane angiography. Ultrasound measurements of the flow rates were performed with perivascular flow probes. Pressures were recorded using intravascular catheters. This data was used as boundary conditions in the commercial code FLUENT® for calculation of the flow field. Our numerical findings are suggestive of strong Dean vortices towards both vein flow exits, verified by color Doppler. The high wall shear stresses that accompany these vortices are related to areas of intimal hyperplasia, as evidenced in preliminary histological studies of the venous vessel wall.**

Manuscript received 12th June, 2008. This paper is part of the 03ED 262 research project, implemented within the framework of the "Reinforcement of Human Research Manpower" (PENED) and co-financed by National and Community Funds (20% from Greek Ministry of Development – General Secretariat of Research and Technology and 80% from E.U. – European Social Fund).

T. A. Manos is with the Laboratory of Biofluid-Mechanics and Biomedical Engineering, National Technical University of Athens, Athens, Greece (e-mail: tmanos@fluid.mech.ntua.gr).

D. P. Sokolis is with the Center of Experimental Surgery, Foundation of Biomedical Research, Academy of Athens, Athens, Greece (e-mail: dsokolis@bioacademy.gr).

A. T. Giagini is with the Center of Experimental Surgery, Foundation of Biomedical Research, Academy of Athens, Athens, Greece (e-mail: atgiag@bioacademy.gr).

J. D. Kakisis is with the Vascular Unit, 3rd Department of Surgery, University of Athens School of Medicine, Attikon University Hospital, Athens, Greece (e-mail: kakisis@yahoo.gr).

C. H. Davos is with the Clinical Research Center, Foundation of Biomedical Research, Academy of Athens, Athens, Greece (e-mail: cdavos@bioacademy.gr).

P. E. Karayannacos is with the Center of Experimental Surgery, Foundation of Biomedical Research, Academy of Athens, Athens, Greece (e-mail: pkarayannacos@bioacademy.gr).

N. Stergiopulos is with the Laboratory of Hemodynamics and Cardiovascular Technology, Swiss Federal Institute of Technology, Lausanne, Switzerland (e-mail: nikolaos.stergiopulos@epfl.ch).

S. Tsangaris is with the Laboratory of Biofluid-Mechanics and Biomedical Engineering, National Technical University of Athens, Athens, Greece (corresponding author, e-mail: tsanga@central.ntua.gr, 0030-210-7721043; fax: 0030-210-7721057).

I. Introduction

The arteriovenous shunt (AVS) is the surgical connection of an artery to a vein through a graft, which is created in hemodialysis patients as an access site. Polytetrafluroethylene (PTFE) is often used as a synthetic graft material for that purpose. Unfortunately, more than half of the arteriovenous (AV) grafts are occluded and fail due to the formation of intimal hyperplasia at the venous side of AVS, so that surgical reconstruction may be necessary within three years [1].

Various factors have been proposed to predispose to graft failure the most important of those being mechanical injury of the host vein, mismatched compliance between graft and vein, and the disturbance of hemodynamic conditions in the region of anastomosis [2], [3].

This paper presents a combined in vivo & numerical study, with the purpose of examining the hemodynamics associated with intimal thickening in AVS. A subject-specific geometry was employed together with boundary conditions obtained from in vivo flow and pressure measurements. The numerical results were correlated with the corresponding color Doppler ultrasound and histomorphological findings. Few are the studies, where this kind of data association has been carried out so far.

II. Materials and Methods

A. Animals

A healthy male Landrace pig weighing 65 kg underwent surgical exposure of the right common carotid artery and ipsilateral internal jugular vein, and creation of an AVS via an expanded (e-PTFE) graft, according to the model by Rotmans et al. [4]. The animal was sacrificed 1 month postoperatively. Animal housing and handling complied with the guiding principles of the American Physiological Society and the Greek Presidential Decree 160/1991, issued after the European Union Directive 609/1986. The experimental protocol was approved by the Ethics Committee of Foundation of Biomedical Research of the Academy of Athens.

B. Surgical Procedures

Starting 6 days preoperatively, the animal received 100 mg/day acetylsalicylic acid (Salospir; Unipharm), 75 mg/day clopidogrel (Plavix; Sanofi Aventis), and 25 mg/day digoxin (Digoxin; Sandoz) until termination, with the latter stopped

on the 8th day postoperatively. On the day of surgery, the animal was fasted overnight and sedated intramuscularly with 10 mg/kg ketamine (Imalgen; Merial), 4 mg/kg azaperone (Suicalm; Jansen-Cilag), and 0.05 mg/kg atropine (Atropine; Demo). Anaesthesia was induced, 15 min later, with intravenous administration of 0.9 mg/kg propofol (Diprivan 1% w/v; AstraZeneca).

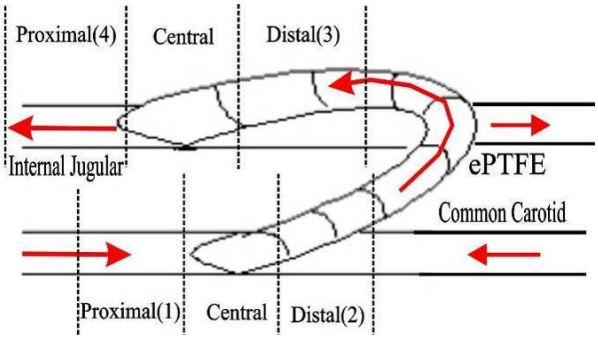

Fig. 1. Schematic representation of AVS via an ePTFE graft between the common carotid artery and internal jugular vein, and the numbering of specimens.

During induction of anesthesia, blood pressure was monitored non-invasively every 3 min and as required with a pressure sphygmomanometer placed at the right front limb of the animal. External ECG leads were placed for monitoring heart rate. The animal was connected to an anesthetic machine (MDS Matrx; Orchard Park, NY, USA) and a volume control respirator (Model 2000; Hallowell EMC, Pittsfield, MA, USA). Sevoflurane (Sevorane; Abbott) 3-5 % (vaporizer setting) in oxygen was administered for the maintenance of anesthesia.

Under sterile conditions, a midline cervical incision was made, and the right common carotid artery and ipsilateral internal jugular vein were exposed. Papaverine (5 mg/ml) was instilled locally to avoid vasospasm. Heparin (iv, 200 IU/kg) was given before manipulation of the vessels. The artery was clamped using atraumatic clamps and an 8-mm arteriotomy was performed. An end-to-side anastomosis was created at a 45º angle using a continuous 8-0 polypropelene suture. A reinforced, thin-walled, ringed, e-PTFE graft of 6-mm diameter and 10-cm length was used (Advanta VS; Atrium Medical Corp, Hudson, NH, USA). The venous anastomosis was created similarly, Fig. 1.

C. *Euthanasia and Tissue Preparation*

Before the animal was sacrificed, it was premedicated and anesthetized as above. The midline neck incision was reopened, and the carotid artery and jugular vein carefully exposed once more. Flow and pressure measurements were conducted as described below. The animal was sacrificed with a bolus dose of pentobarbital sodium, and the anastomosed and control tissues were cautiously excised to avoid damage to their walls. The contralateral internal jugular vein served as control. For both cases, the adherent connective tissue was carefully trimmed and the specimens were prepared for the histomorphometrical study.

D. *Hemodynamic Measurements*

All necessary measurements used for the CFD model were obtained 1 month after graft implantation. The flow field at the anastomosis was inspected preoperatively with the cardiovascular color flow Doppler ultrasound system (Vivid 7; GE Medical Systems, Milwaukee, WI, USA), using its linear array vascular probe (size 12L) at color and pulse wave Doppler modes. Blood flows at the proximal (position 1) and distal (position 2) artery, and at the proximal (position 3) and distal (position 4) vein were measured using perivascular ultrasonic flow probes (TA 420; Transonic Systems, Ithaca, NY, USA) of appropriate size, Figs. 1-3.

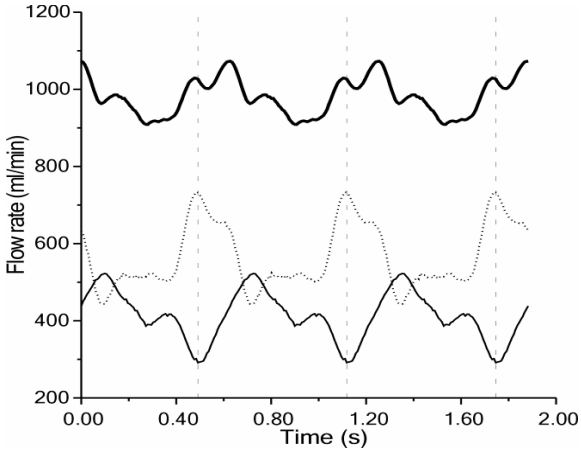

Fig. 2. Processed recordings of flow rate at the proximal (position 1) carotid artery (dotted line), at the distal (position 2) carotid artery (bottom thin line), and at the graft (top thick line).

Blood flow was recorded first at the vein and then at the artery, because of shortage in appropriate probe sizes. Pressure was recorded simultaneously with the flows, only in the artery. Recordings were performed under a hemodynamically stable condition; presumably when pressures and flows did not exhibit temporal variations for about 5 min. This practically meant waiting for 10 min if no vasospasm was apparent or 30 min otherwise. All data signals were simultaneously recorded by a digital acquisition system (Sonometrics System; Sonometrics Co, Ontario, Canada) at 60-sec data epochs with a sampling rate in excess of 300 Hz, during which the respirator was turned off to avoid respiration-induced noise. Afterwards, the flow field at the anastomosis was inspected once more with the cardiovascular ultrasound system; with the image acquisition made intraoperatively by use of the linear array cardiac probe (size i13L). Pressure at the proximal vein was determined with a 5F catheter-tipped pressure transducer (SPC-450; Millar Instruments, Houston, TX, USA), Fig. 3.

E. *Biplane Angiography*

Subsequent to exposure of the carotid artery and jugular vein, and to hemodynamic measurements, biplane angiography

was carried out using a C-arm mobile diagnostic X-ray image acquisition and viewing system (BV Libra; Philips Medical Systems, P.M.G. Surgery, The Netherlands). A catheter was inserted into the graft. The C-arm was tested at various angles to avoid adjustments during image acquisition. Contrast media was then administered and digital subtraction angiography was performed at three selected angles, allowing unambiguous identification of the venous anastomosis. The monitor output was recorded on DVD, Fig. 4 (left).

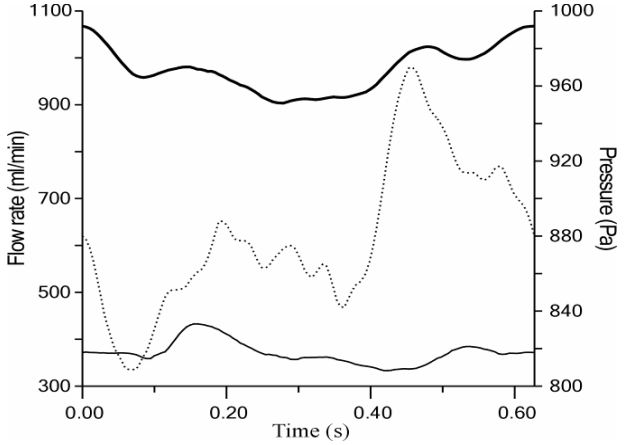

Fig. 3. Processed recordings of flow rate at the graft inlet (top thick line), of pressure (dotted line) at the distal outlet (position 3), and of flow rate (bottom thin line) at the proximal outlet (position 4).

F. Histomorphometrical Studies

Following animal euthanasia, tissue from the region of venous anastomosis was removed and cut into three parts of equal length: the central, proximal, and distal to the anastomosis tissue segments, Fig. 1.

Specimens from the three regions were fixed with 10% buffered formalin over 24 hours, dehydrated in graded ethanol and xylol, and embedded in paraffin wax. Serial 5-μm thick sections were cut on a microtome (Leica RM 2125; Leica, Nussloch, Germany) and treated with picro-Sirius red for collagen matrix and orcein for elastin fiber staining.

Images were taken by a digital camera (Altra 20; Soft Imaging System, Muenster, Germany) fitted to a light microscope (Olympus CX31; Olympus, Tokyo, Japan) and processed using a commercial image-analysis software (Image-Pro Plus v.6.0; Media Cybernetics Inc, Silver Spring, MD, USA). The thickness of tunica intima, media, and adventitia, and the entire vessel wall was measured. Elastin and collagen area densities for the three layers were also measured after the micrographs were segmented using the software. These were calculated with respect to the total area of that layer in the region of interest. The area densities for the entire vessel were calculated using the respective ones for the three layers, and their thicknesses. Values for each specimen were averages from three sections.

G. Postoperative Data Editing and Analysis

The data stored in the Sonometrics console was used as boundary conditions after careful editing. The flow rates at the proximal and distal carotid artery were added to obtain the graft inlet flow. The same was done for the proximal and distal jugular vein. Pressure and flow signals were delineated according to cardiac cycle. Synchronization of the two recordings was performed by a reference signal, i.e. the flow through the graft. A characteristic cardiac pulse was selected and extracted in ascii format for further processing. Data analysis was carried out with the Sonosoft software (Sonometrics Co).

Next to importing the pulse data in Excel (Microsoft Office Excel 2003), all signals were filtered to remove the linear drift caused by the temporal variation of hemodynamics at the anastomosis. The flows were also adjusted to account for the relative difference, because of the probe accuracy, Fig. 2 and Fig. 3.

From the modified signals, we selected the graft and distal vein flow, and the proximal vein pressure for processing in MATLAB, because these were used as boundary conditions for our models. This data was first re-sampled based on a common time vector, and then smoothed and curve-fitted using a Fourier fit of eighth degree. Subsequently, a user defined function (UDF) was written in C, which defines the pressure and flow for every time step. The C program was used as input for the unsteady numerical simulation.

H. Reconstruction of Geometry and Mesh Development

The three angles, at which the monitor output was recorded, were studied and appropriate images were selected for geometrical reconstruction. Using the Info Cliper software (Canopus Co, Reading, UK), images of interest were captured in bmp format. In the case studied, the venous anastomosis was planar and its plane was perpendicular to the surgical table, simplifying the reconstruction. There was no need for a reconstruction algorithm; only one image at an axis vertical to the plane of anastomosis was required, Fig. 4 (left).

The selected image was rotated, filtered, and segmented using the Image-Pro Plus software. Then, the vessels centerline and boundaries were traced manually by point selection with Paint Shop Pro 5 (Jasc Software Inc, Eden Prairie, MN, USA). This modified image was processed by a developed MATLAB code, which extracted the coordinates of the points selected. The point cloud was then imported into GAMBIT (v.2.3.16; Fluent Inc, Lebanon, NH, USA). The three dimensional geometry was reconstructed assuming circular cross-sections of varying diameter for the graft and vessel. The model was first cut in the middle, taking into account the planar symmetry, which aided to decrease the total number of elements. Afterwards, the geometry was split into four regions: the junction, proximal venous segment (PVS), distal venous segment (DVS), and graft inlet. In the junction, an unstructured grid was

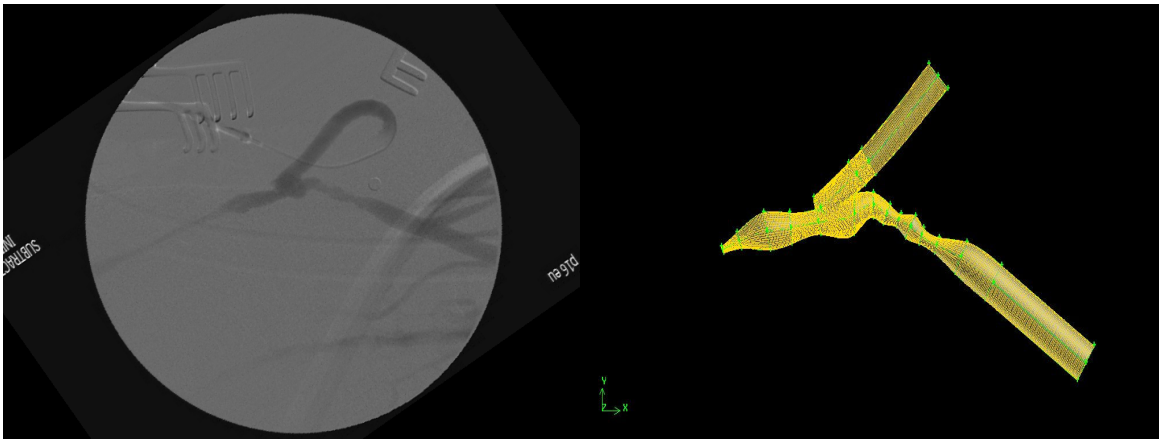

Fig. 4. Angiography of graft – jugular vein anastomosis (left) and 3D mesh of the anastomosis generated by GAMBIT (right) of the selected cardiac cycle, based on the curve fits.

used that consisted of wedge, tetrahedron and pyramidal elements, while for the other three volumes a structured grid with hexahedron elements was used, Fig. 4 (right). The total element count was 173177.

I. Numerical Simulation

The mesh generated was exported in the appropriate format to the finite volume solver Fluent (v.6.2.16; Fluent Inc, Lebanon, NH, USA). Blood was approximated as a Newtonian fluid with a viscosity of 3.6×10^{-3} Pa·s and a density of 1000 kg/m^3. Flow was assumed to be laminar and pulsating. The processed recordings of pressure and flows, displayed in Fig. 3, were considered as boundary conditions. At the graft inlet and proximal venous outlet (position 4), pulsatile entrance velocities with plug profiles were applied, whereas for the distal outlet (position 3) the time dependent pressure waveform was used. The boundary condition temporal variation was set according to the aforementioned UDF, which was connected to the solver. The mean flow rate was 980 ml/min, which corresponds to a mean graft inflow velocity of 0.47 m/s or a mean Reynolds Number of 870, based on the graft inlet diameter, whereas the highest Reynolds number was 952. The pulse period, about 0.63 s (heart rate of 95 bpm), was divided into 100 time steps, while three pulse cycles were initially simulated to eliminate transient artifacts.

The Navier-Stokes equations were solved by using a segregated solver with a first-order implicit unsteady formulation, while for the pressure discretization a PRESTO! scheme and for the momentum a first-order upwind scheme were used. The pressure-velocity coupling method of choice was the PISO algorithm. The convergence criteria, defining the end of iterative process, were continuity and momentum residuals of 0.0001.

III. Results

A. Numerical Simulation Results

The flow patterns observed were complex and highly three dimensional, due to the complex geometry of AVS one month after its creation. In Fig. 5 the contours and in Fig. 6 velocity vectors are shown at the symmetry plane of the model geometry. From these figures, the following may be deduced: Flow enters the graft as a plug velocity profile, but as approaches the host vessel it becomes fully developed. Part of the flow, before entering the junction region, collides with the wall of the bulge that is present near the toe section and a recirculation zone evolves at that point. In contrast, the main part of flow strikes the floor of the host vessel and separates into two streams of opposing directions. A stagnation point is formed at the point of division.

Following that part of the stream, heading towards the PVS exit (position 4), we notice that as it turns on the flow dividing wall, it sets up a Dean flow pattern in which flow on the lateral walls moves upwards towards the toe, Figs. 7. These counter rotating vortices have their center near the toe wall at the start, but as they move downstream their center approaches the vessel axis. At the PVS exit (position 4), there is a vessel contraction, where the vessel lumen has it smallest cross sectional area. Maximum flow velocities ranging from 4.9 to 5.0 m/s, during the heart cycle, are noted there. The flow field pattern did not display significant temporal variation.

The other part of inlet flow, which divides at the stagnation point region, moves towards the distal exit (position 3). This stream also forms Dean vortices, accompanying it until it reaches the exits, but with a diminishing effect. This venous segment exhibits two stenotic regions lying close to each other. The first stenosis creates a strong jet stream that passes through the expansion zone between the two stenoses and enters the final one. High velocities between 1.8 and 2.3 m/s were detected at these stenotic areas. The two expansion zones cause flow

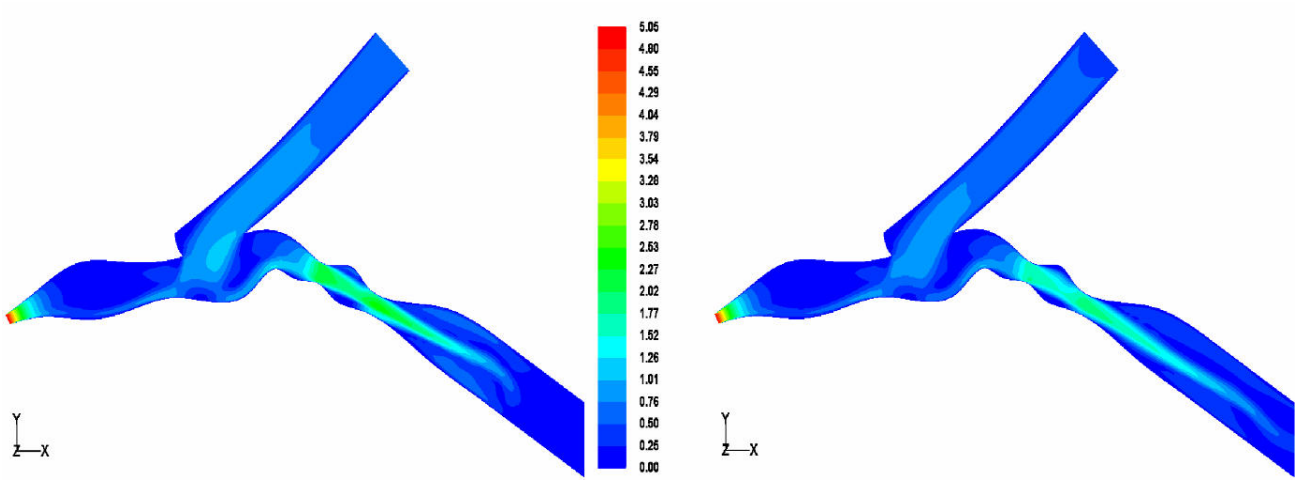

Fig. 5. Contours of velocity magnitude at the symmetry plane displaying the flow division and the distal jet. Maximum flow rate (left); Minimum flow rate (right).

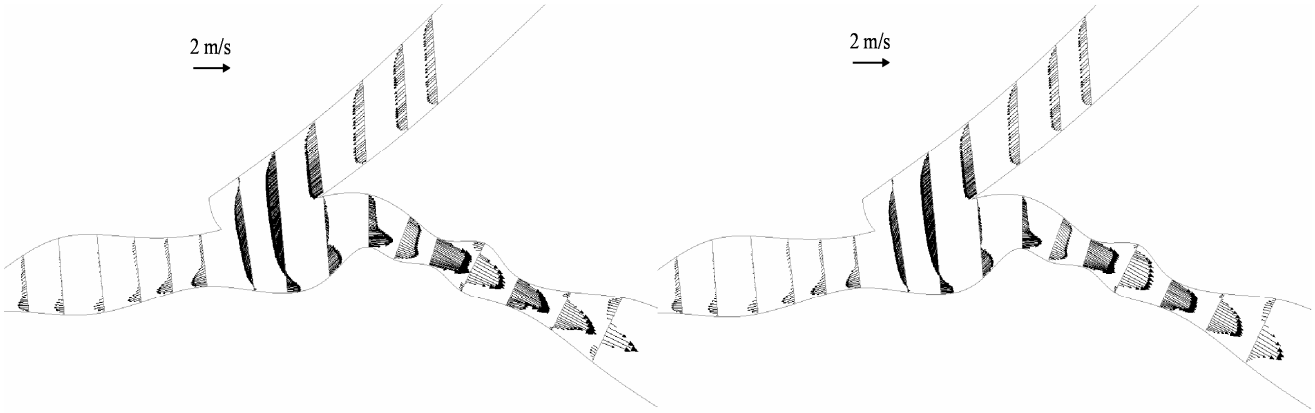

Fig. 6. Vectors of velocity at the symmetry plane that illustrate the existence of recirculation zones in the DVS. Maximum flow rate (left); Minimum flow rate right).

separation and as a consequence recirculation zones form, which change during the heart cycle. For the minimum graft inlet flow the jet is longer and produces a large recirculation zone with combined Dean vortices on the top of the second expansion area, whereas at the bottom a simple recirculation region appears of much smaller scale (Fig. 7-8 right). In contrast, for the maximum inlet flow the jet is shorter, but has higher velocities, causing two extended recirculation zones, but with Dean flow apparent only for the bottom one, which again is the smallest of the two (Fig. 7-8 left).

Wall shear stress (WSS) contours for the junction region are displayed in Fig. 9 for the maximum (left) and minimum (right) flow cases. The mean value for WSS of the model is 6.0-7.5 Pa, consistent with the value reported by Harugushi et al [3]. The maximum value was found at the stenosis of the proximal exit (position 4), between 680 and 696 Pa. Other regions of high WSS were the first, i.e. 93-124 Pa, and second stenosis, i.e. 68-89 Pa, of the distal part, the floor of DVS opposite to the heel region, i.e. 33-49 Pa, and finally the region around the stagnation point on the lateral walls of the host vessel, i.e. 27-31 Pa.

The range of values for the WSS, mentioned above, together with Fig. 9 illustrate a regional difference in temporal variation between the PVS and DVS. The PVS and junction region exhibit slight changes in WSS, in contrast to the DVS, where higher alterations are noted, especially on the venous floor opposite the heel. The difference is caused by temporal change in flow division, during the heart pulse. For minimum inlet flow, a 44:56, whereas for the maximum flow a 38:62 PVS:DVS flow split was observed. This means that as graft flow increases more blood is channeled away from the PVS, which is partially occluded. As a result the flow rate increase, defining the WSS variation, is 2% and 28% for the proximal and distal venous segment, respectively. This also means that the distal region is subjected to higher temporal WSS gradients.

B. Histomorphometrical Results

Table 1 shows the histomorphometrical results of our study. Of the three vessel layers examined, the changes found in tunica intima and media were most significant, the reason being that these layers were affected to a greater

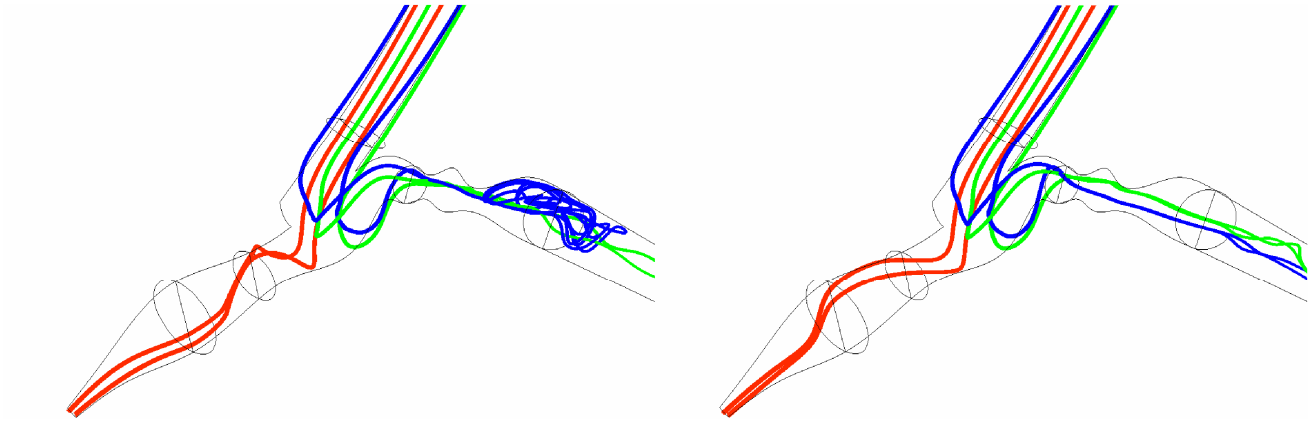

Fig. 7. Pathlines of six particles showing the Dean flow motion for maximum (left) and minimum (right) graft inlet flow rates.

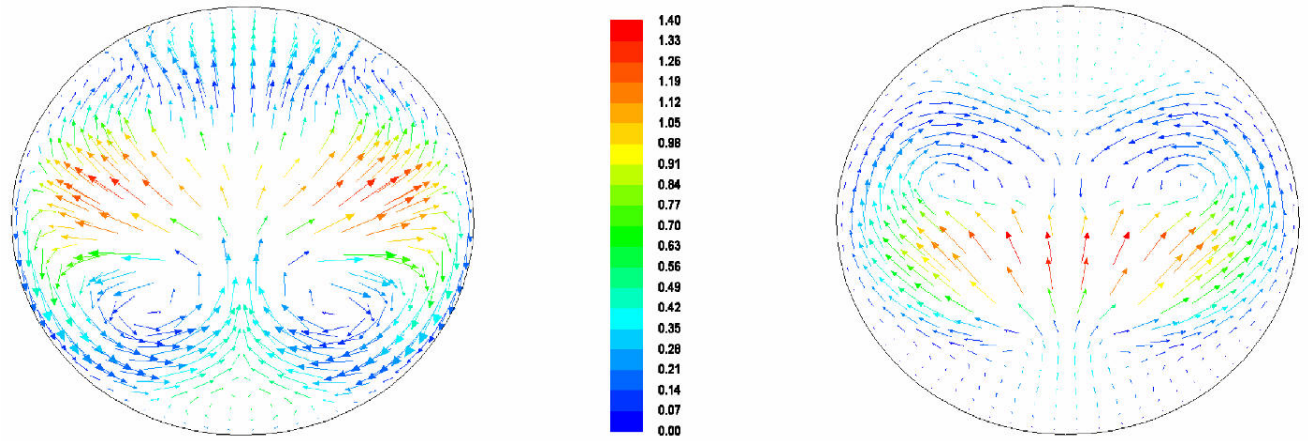

Fig. 8. In plane velocity vectors displaying the secondary flows at a cross-section of the second expansion region situated in the DVS. Maximum inlet flow rate (left); Minimum inlet flow rate (right).

extent by the disturbed flow, owing to their close proximity to it.

After a close inspection of the table, we deduce that there is an increase in thickness of all layers at all positions of the anastomosis compared to control, except for a single case. The adventitia exhibits small variations, while for the other two layers there is profound increase in thickness, which attests to the fact that intimal hyperplasia is present [7], [8]. For tunica intima, a ten-fold thickness increase is noted at the DVS and a three-fold increase at the proximal one. Thickness variation is much smaller at the central segment. The opposite is true for tunica media, where the greatest change is found at the central region.

Concerning the elastin area density, there is a decrease in the anastomosed compared to control tissue in all cases. This is in agreement with the literature, according to which areas of high velocities and WSS are correlated with a decrease in elastin content [7], [9]. At some instances, the variation is slight while at others elastin content is less than half compared to control values, as in the PVS. Collagen results are less definite. In half of the cases there is collagen content increase in anastomosed tissue, while for the other half the opposite is true.

TABLE I
HISTOMORPHOMETRICAL RESULTS AND THE ANASTOMOSED AND CONTROL TISSUE

		Intima	Media	Adventitia	Total
Vessel wall thickness (μm)					
Anastomosis	Proximal	34.0 ± 0.6	381.6 ± 2.2	339.0 ± 0.5	760.5 ± 2.7
	Central	20.0 ± 0.7	329.5 ± 7.0	105.4 ± 2.0	454.9 ±4.9
	Distal	309.4 ± 17.6	194.4 ± 8.5	399.1 ± 5.0	902.9 ± 23.0
Control	Proximal	15.0 ± 1.1	131.7 ± 10.4	181.9 ± 10.4	328.5 ± 6.2
	Central	15.1 ± 1.4	59.2 ± 3.4	131.5 ± 7.4	205.9 ± 7.9
	Distal	28.0 ± 2.0	138.2 ± 9.7	275.5 ± 13.2	441.7 ± 18.3
Collagen area density (%)					
Anastomosis	Proximal	18.1 ± 0.7	23.5 ± 0.9	21.4 ± 1.0	22.3 ± 0.2
	Central	16.8 ± 0.7	13.4 ± 0.7	17.8 ± 0.6	14.5 ± 0.5
	Distal	13.4 ± 0.6	13.8 ± 0.7	20.0 ± 1.4	16.4 ± 0.8
Control	Proximal	25.8 ± 0.7	12.6 ± 0.7	17.9 ± 0.7	16.2 ± 0.7
	Central	8.5 ± 0.9	12.5 ± 0.6	17.0 ± 1.0	15.0 ± 0.6
	Distal	21.7 ± 1.1	14.5 ± 0.7	21.5 ± 1.1	19.4 ± 0.9
Elastin area density (%)					
Anastomosis	Proximal	8.3 ± 0.5	7.0 ± 0.6	8.5 ± 0.6	7.8 ± 0.4
	Central	10.2 ± 0.4	5.0 ± 0.2	8.3 ± 0.4	6.0 ± 0.1
	Distal	4.4 ± 0.4	6.2 ± 0.5	9.7 ± 0.6	7.2 ± 0.5
Control	Proximal	15.5 ± 0.6	9.5 ± 0.3	12.5 ± 0.6	11.4 ± 0.4
	Central	13.9 ± 0.1	6.0 ± 0.1	14.8 ± 0.2	12.2 ± 0.3
	Distal	12.0 ± 0.5	13.5 ± 1.5	15.3 ± 0.7	14.5 ± 0.8

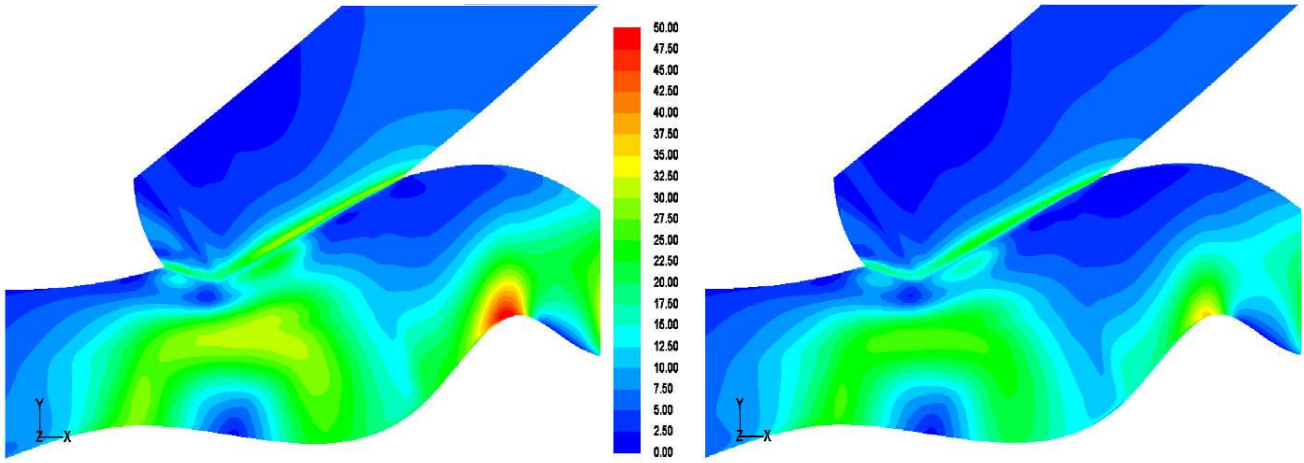

Fig. 9. Contours of WSS, which emphasize on the large temporal increase seen opposite of the heel. Maximum inlet flow rate (left); Minimum inlet flow rate (right).

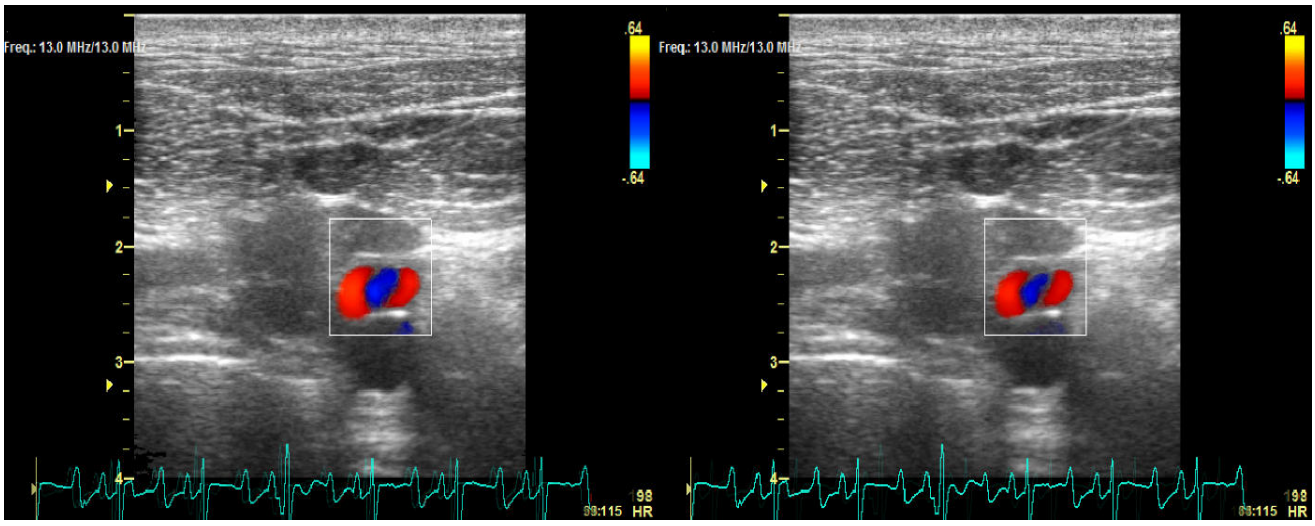

Fig. 10. Dean vortices at cross-sections obtained trancutaneously by color Doppler ultrasound. The color demonstrates the direction of the velocity components which are parallel to the view plane. The red color exhibits flow towards, whereas blue flow away from the probe. Maximum inlet flow rate (left); Minimum inlet flow rate (right).

C. *Ultrasound Results*

The Dean vortices were noticed in the preoperative Color Doppler recordings (Fig. 10) as three consecutive stripes of alternating colors (red-blue-red). These images were obtained by placing the probe on the swine neck, vertically to surgical table. The middle stripe could not be mistaken with a recirculation zone, because it extended from one side of the vessel lumen to the other. The intraoperative ultrasound data did not illustrate the existence of counter rotating vortices with such clarity, because there was vasospasm combined with flow distortion due to the probe pressing on the vessel wall.

IV. Discussion

The flow in the anastomosis junction was highly complex and exhibited many features not reported in previous studies. The reason most likely is that the geometry was subject-specific, based on the angiography taken from a porcine AVS one month post-implantation. This meant that the vessel studied had remodeled and intimal hyperplasia had developed, distorting the initial geometry. The patient-specific geometry examined had many irregularities. These were: a) the bulge at the toe area, b) the stenosis at the PVS exit, and c) the stenoses at the DVS. The bulge might have been caused by the way the graft had been sutured and by intimal hyperplasia, owing to the resulting disturbed flow. For the other two vessel formations, intimal hyperplasia must have been again the reason. It is known fact that at the PVS of AV grafts there is an extended toe and floor region, where hyperplasia is noted [2], [3]. The reasons incriminated for its development are high WSS and high WSS gradients [3]. Our numerical results confirmed those findings at the far PVS, but not at the toe region. In contrast to the literature, the DVS did

also exhibit high WSS. We believe that this may be reminiscent of the fact that after constriction of the PVS, the flow in the distal one increased, eliciting high WSS.

Our histomorphometrical results suggested that the DVS close to the heel was affected the most. At this region, there is a ten-fold increase in thickness of tunica intima, validating the existence of intimal hyperplasia. The elastin content of that region also varied significantly, as values were less than half the ones found for control. Both alterations in vessel structure are correlated with high WSS in the literature [3], [4], [8], [10], [11]. The numerical simulation performed in this study showed that the highest WSS of the junction region were found at the host vessel floor opposite to the heel, at the DVS. This observation may be related to the increased wall thickness and decreased elastin content.

The most interesting flow features noted were the Dean vortices that developed in both segments. These counter rotating vortices have been also noted in other numerical studies [1], [6] for the PVS, although the geometry and flow conditions were different. The same is not true for the Dean flow noticed at the DVS. The existence of these vortices in the anastomosed jugular vein was validated by color Doppler ultrasound (Fig. 10).

The flow unsteadiness caused a significant change only to the DVS hemodynamics. The PVS flow rate did not demonstrate the expected increase. Although the graft showed a 17% increase, the PVS increased only by 2%, because the flow was channeled towards the other side of the anastomosed jugular vein. Consequently, the DVS showed the highest velocities, WSS, and temporal WSS gradients in the proximity of the junction region.

Another interesting finding of this study was the decreased graft flow pulsatility, compared to the expected one, obtained from the addition of the two recorded carotid flows (Fig. 2). Although the proximal and distal carotid flows had in turn amplitudes of 290 and 230 ml/min the graft flow variation was only 160 ml/min, because the two signals were 180^{o} out of phase, so that the maximum observed in the first was diminished by the simultaneous minimum seen in the second. The difference in phase can be explained by the fact that the proximal carotid flow came directly from the heart, whereas the distal one passed through the circle of Willis before reaching the AVS.

There are limitations with the present numerical study. The vessel wall distensibility was ignored and the fluid was assumed to be Newtonian, which is a good approximation for large vessels. Furthermore, the geometry portrayed the remodeled vessel, just prior to the loss of patency; so that we examined the result of disturbed flow.

ACKNOWLEDGMENT

The authors thank: C. A. Dimitriou for his technical support throughout the project, E. Varela for her assistance with the U/S scanning, and M. Peroulis and M. Katsimpoulas for their aid and suggestions with the surgical procedure.

REFERENCES

[1] F. Loth, P. F. Fisher, N. Arslan, C. D. Bertram, S. E. Lee, T. J. Royston, W. E. Shaalan and H. S. Bassiouny, "Transitional Flow at the Venous Anastomosis of an Arteriovenous Graft: Potential Activation of the ERK1/2 Mechanotransduction Pathway," *J. Biomech. Eng.*, Vol. 125, pp. 49-61, 2003.

[2] F. Loth, P. F. Fischer and H. S. Bassiouny, "Blood Flow in End-to-Side Anastomoses," *Annu. Rev. Fluid Mech.*, Vol. 40, pp 367-393, 2008.

[3] H. Haruguchi and S. Teraoka, "Intimal hyperplasia and hemodynamic factors in arterial bypass and arteriovenous grafts: a review," *J. Artif. Organs.*, Vol. 6, pp. 227-235, 2003.

[4] J. I. Rotmans, E. Velema, H. J. M. Verhagen, J. D. Blankensteijn, J. J. P. Kastelein, D. P. V. de Kleijn, M. Yo, G. Pasterkamp and E. S. G. Stroes, "Rapid, Arteriovenous Graft Failure Due to Intimal Hyperplasia: A Porcine, Bilateral, Carotid Arteriovenous Graft Model," *J. Surg. Res.*, Vol. 113, pp. 161-171, 2003.

[5] K. Hayashi, K. Mori and H. Miyazaki, "Biomechanical response of femoral vein to chronic elevation of blood pressure in rabbits," *Am. J. Physiol. Heart. Circ. Physiol.*, Vol. 284, pp. H511-H512, 2003.

[6] J. Chen, X. Y. Lu and W. Wang, "Non-Newtonian effects of blood flow on hemodynamics in distal vascular graft anastomoses," *J. Biomech.*, Vol. 39, pp. 1983-1995, 2006.

[7] J. I. Rotmans, E. Velema, H. J. M. Verhagen, J. D. Blankenstejin, D. R. V. Kleijn, G. Pasetrkamp and E. S. G. Stroes, "Matrix metalloproteinase inhibition reduces intima hyperplasia in a porcine arteriovenous-graft model," *J. Vasc. Surg.*, Vol. 39, pp. 432-439, 2004.

[8] R. Tran-Son-Tay, M. Hwang, S. A. Berceli, C. K. Ozaki and M. Garbey, "A model of vein graft intimal hyperplasia," *Conf. Proc. 29th Annual Internat. Conf. of IEEE Eng. Med. Biol. Soc.*, Lyon, France, pp. 5807-5810, 2007.

[9] S. Misra, D. A. Woodrum, J. Homburger, S. Elkouri, J. N. Mandrekar, V. Barocas, J. F. Glockner, D. K. Rajan and D. Mukhopadhyay, "Assessment of Wall Shear Stress Changes in Arteries and Veins of Arteriovenous Polytetrafluoroethylene Grafts Using Magnetic Resonance Imaging," *Cardiovasc. Intervent. Radiol.* Vol. 29, pp. 624-629, 2006.

[10] J. J. Wentzel, E. Janssen, J. Vos, J. C. Schuurbiers, R. Krams, P. W. Serruys, P. J. de Feyter and C. J. Slager, "Extension of increased atherosclerotic wall thickness into high shear stress regions is associated with loss of compensatory remodeling" *Circulation*, Vol. 108, pp. 17-23, 2003.

[11] L. Hofstra, D. C. Bergmans, K. M. Leunissen, A. P. Hoeks, P. J. Kitslaar, M. J. Daemen and J. H. Tordoir, "Anastomotic intimal hyperplasia in prosthetic arteriovenous fistulas for hemodialysis is associated with initial high flow velocity and not with mismatch in elastic properties," *J. Am. Soc. Nephrol.*, Vol. 6, pp. 1625-1633, 1995.